Application of Bidimensional Empirical Mode Decomposition for Particle Identification and Size Determination

DIANA RUBIO, NICOLAS SASSANO, MARCELA MORVIDONE, ROSA PIOTRKOWSKI
ITECA (UNSAM-CONICET), CEDEMA
Universidad Nacional de San Martin
25 de Mayo y Francia, 1650 San Martin, Buenos Aires
ARGENTINA

Abstract: - The analysis of surface texture appears in different disciplines of science and technology. Surface texture is generally multiscale and can be separated into different spatial frequency or wavelength ranges providing information on image characteristics such as shape, roughness, pseudoperiodic components and chaotic components. Surface texture translates into image texture. Textures in images are complex visual patterns composed of entities or subpatterns that have characteristic brightness, color, slope, size, etc. In this work, we address the analysis of multimodal images and their decomposition using the bidimensional empirical mode decomposition. This approach allows us to obtain component images from each original image, each of them with a spatial frequency range. These analysis methods are currently used in images from various disciplines such as biology (analysis of biological tissues), environmental and health sciences (particulate matter dispersed in the atmosphere), materials sciences (texture on surfaces), earth sciences (SAR images). The main objective is to present an algorithm that allows identifying, segmenting, and classifying structures and morphologies in each image mode. The proposed numerical technique is applied to images from cytology analysis to study number of particles present in fibroma (benign tumor) nuclei compared to the number in sarcoma (malignant tumor) nuclei in order to investigate if there is a significant difference between them, sufficient to use this fact as part of a diagnosis.

Key-Words: - Bidimensional Empirical Mode Decomposition, Texture Analysis, Particle Size, Particle Asymmetry, Cytology Analysis, Fibrosarcoma.

Received: May 29, 2024. Revised: August 6, 2024. Accepted: September 7, 2024. Published: October 24, 2024.

1 Introduction

Properly characterizing the final structures has an undoubted impact on applications. For example, it helps to make better decisions in manufacturing processes in the case of materials and to better measure the consequences in the case of pollution.

Multiscale methods and algorithms such as bidimensional wavelet transform and bidimensional empirical mode decomposition, applied to surfaces and images are constantly evolving. Their optimization leads to representing the information in a simpler, more accurate and precise way.

Empirical Mode Decomposition (EMD) was pioneered by Huang et al. in 1989, for one dimension, and it has proven to be a successful tool for analyzing non-stationary and nonlinear time series. This method finds application in diverse fields such as acoustic emission studies and climate analysis, where traditional linear methods may fall short. Time series are decomposed into a finite number of zero-mean components called Intrinsic Mode Functions (IMFs) and a residue, where the number of IMFs depends on the signal. Each IMF represents an oscillating function that optimally captures the signal's characteristics, allowing for the identification of underlying physical processes. The Hilbert Transform applied to each IMF enables the determination of instantaneous frequency, contributing to the overall Hilbert-Huang Transform (HHT) procedure. These IMFs form a complete a posteriori basis and are empirically derived from the original series. Moreover, the residue, a monotonous function, provides insight into the series' overall trend. Beyond EMD, advancements like Ensemble Empirical Mode Decomposition (EEMD) and Variational Mode Decomposition (VEMD) have further expanded its utility across various domains. The decomposition strategies are varied and adapted to different purposes. One of the authors, R.P., has been actively engaged in diverse applications, including the evaluation of material damage via acoustic emission analysis, investigation of

electrocardiograms (ECG) for ischemia detection and examination of climate-related data [10]. In 2003, Nunes *et al.* [11] extended EMD to BEMD for analyzing image texture. Since then, BEMD and bidimensional wavelet transform methods continue evolving.

In [1], Clausel *et al*. introduced a two-dimensional version of the synchrosqueezed wavelet transform, which extends the concept of analytical signal to images. Kim *et al.* [7] proposed the two-dimensional statistical empirical modal decomposition (BSEMD) algorithm, which employs an alternative smoothing procedure for constructing 2D upper and lower envelopes instead of interpolation. In [17], Xie *et al.* presented optimization approaches based on Delaunay triangulation of local maxima (minima) and scale, using the initial modal image to effectively capture multiscale features of input images. Ding *et al*. [4] utilized a wavelet transform in combination with a deep neural network to establish a one-to-one correspondence of semantic structures in images, thereby avoiding artificial style transitions around these structures. In [13], Oyelade *et al.* addressed image degradation issues and improved image quality through a wavelet transform-based algorithm. They reconstructed images using diffuse contrast enhancement to highlight details while preserving spectral information.

These methodologies are employed in sophisticated applications of science and technology dedicated to texture analysis and they represent a dynamic and continually evolving research domain. In [15], Shao *et al.* analyzed surface topography by extracting encrypted surface components using a two-dimensional empirical wavelet transform. In [16], Veluppal *et al*. conducted entropy-based multiscale two-dimensional texture analysis to identify texture alterations induced by Alzheimer's disease in brain MRI images. In [18], Yang *et al.* employed BEMD and multifractal geometry to analyze retinal images for detecting various degrees of diabetic retinopathy. Dong *et al*. [5] utilized multiscale models to estimate the effective thermal conductivities of particulate compounds with complex microstructures. In [6], Gogolewski employed fractional spline wavelets to analyze the surface texture of industrial parts across various scales, facilitating the generation of surface profiles with a variable distribution of irregularities. In [19] Yu *et al.* proposed a computer vision-based method for measuring drill edge wear, incorporating an adaptive contrast enhancement algorithm based on two-dimensional local mean decomposition, which groups in similarities in each image mode.

In this work we address the analysis of multimodal images and their decomposition using the BEMD applied to cytology images with the objective to analyze differences in the structure of the nuclei of benign and malignant tumors.

2 Formulation and Methodology

Real-world images often exhibit significant heterogeneity, representing diverse scales and morphologies. Consequently, employing a decomposition method to characterize the various component images becomes both useful and necessary. BEMD stands out for its versatility and adaptability to such diverse data.

The algorithm scheme is sketched in Fig. 1. and then summarized in Sub-Section 2.3.

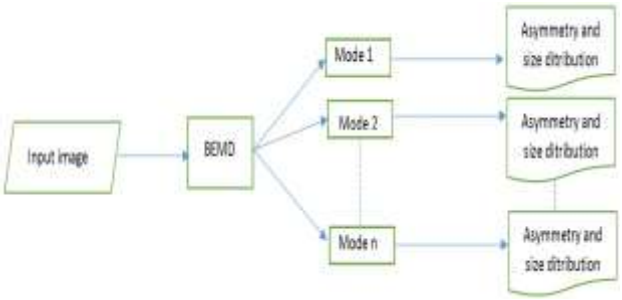

Figure 1. Algorithm scheme.

BEMD enables the extraction of component images, called Bidimensional Intrinsic Mode Functions (BIMF) that contain image information ranging from high frequency to low frequency, along with a residue that is a non-zero mean remainder. After the BEMD is performed on the image, one proceeds to identify particles or structures within these components and classify them based on their size and morphology. Finally, statistical analysis could be eventually conducted to further examine and understand the diverse characteristics present.

The proposed approach was applied to images from cytology studies, where a benign tumor (neurofibroma) and a malignant tumor (fibrosarcoma) were identified by one of the authors, the veterinary N.S., and later confirmed by a pathologist.

Quantifying the difference in number of particles present in fibroma and sarcoma nuclei, could help to obtain clues for further diagnosis and treatment planning. One expects to have robust statistical information in future work.

2.1 Multiscale Decomposition

The BEMD method is applied to images that undergo a decomposition process analogous to its one-dimensional counterpart. BEMD spatial

decomposition enables the extraction of meaningful information from the data in both dimensions simultaneously. By decomposing the image into BIMFs, BEMD unveils intricate patterns and structures that might remain unseen in the original, often complex image, serving as a powerful tool for uncovering hidden spatial features and enhancing our understanding of multidimensional data.

2.2 Particle identification and Size Determination

Once the image (matrix) has been decomposed into BIMFs, the particles, or structure elements, can be identified by locating the local maximum values within each of these matrices. Subsequently, for every detected particle, its size is determined by assessing the local minimum values along the horizontal and vertical direction from each local maximum. This process yields four values, denoted as r_1, r_2, r_3 and r_4, as illustrated in Fig.2. Note that, since the particles are randomly oriented, these values are of statistical nature.

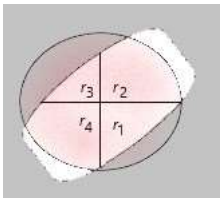

Figure 2: Size determination proposed in the algorithm.

The particle diameter and asymmetry are defined as

$$d = 2\max\{r_1, r_2, r_3, r_4\} \quad (1)$$

$$A = \frac{|dH - dV|}{\max\{dH, dV\}} \quad (2)$$

where

$$dH = r_2 + r_4\,, \quad dV = r_1 + r_3\,. \quad (3)$$

2.3 The Algorithm

For a 2D image *I*, the proposed algorithm consists in the following steps:

1) Initialize $r = I$ (residue) and define $h=I$, $m=0$ (mode).
2) Identify all extrema of *h*.
3) Interpolate extrema that verify the criterion to obtain an upper and lower envelope, namely E_{max} and E_{min}, respectively.
4) Compute the envelope mean E_M.
5) Subtract the mean E_M from the image $h = h - E_M$.
6) Repeat steps 2-5 until *h* can be considered as zero-mean.
7) $m=m+1$, $\text{BIMF}_m = h$, $r = r - h$, $h = r$.
8) Repeat steps 2-7 until the number of extreme values in *r* is less than 2.
9) Determine all local maxima, namely Max, in BIMF_{mode}. Each local maximum corresponds to a particle in BIMF_{mode}.
10) For each local maximum in Max
    a. Find r_1: the closest local minimum below, r_3: the closest local minimum above, r_2: the closest local minimum to the right, r_4: the closest local minimum to the left.
    b. Define the particle size as
    $$d = 2\max\{r_1, r_2, r_3, r_4\}.$$
    c. Define $dH = r_2 + r_4$, $dV = r_1 + r_3$, and the particle asymmetry as
    $$A = \frac{|dH - dV|}{\max\{dH, dV\}}.$$
11) Repeat 9)-10) for the significant modes.

Note that steps 1)-8) are based on Nunes et al. [12] and its implementation is given in [14].

3 Application to Cytology Images

In veterinary medicine, cytology is valuable for morphological cellular diagnosis, relying on microscopic characteristics of cells and extracellular components from various biological samples. It complements clinical diagnosis, which considers the patient holistically alongside all available methods. The aim is to identify at least 80% of cells in preparations, discerning quantities, proportions, and relationships between cells. Thus, cytology can be conclusive, suggestive, or inconclusive in diagnosis. In recent years, there has been an increased demand for cytology diagnosis, especially in skin lesions of domestic canines and felines, due to skin accessibility. Cytology involves microscopic examination of cells from healthy tissues, lesions, or body fluids [2,3,9].

The main objective of cytology is to differentiate between inflammatory and non-inflammatory processes and sometimes between benign and malignant neoplasms within non-inflammatory processes.

There are general and nuclear criteria of malignancy to characterize non-inflammatory processes. The general criteria for malignancy allow the assertion of the presence of reactive cells, meaning cells that have undergone morphological changes. If most cells do not exhibit general criteria of malignancy, the process can be classified as benign. Nuclear criteria of malignancy allow the assertion of the presence of a neoplasm. Neoplastic processes are categorized based on cellular

characteristics. In this sense, four main groups are distinguished: epithelial cell tumors; round cell tumors; naked nuclei neoplasms; mesenchymal cell tumors.

In most malignant processes, a large proportion of cells exhibit pleomorphism in shape, cell size, and nuclear size when comparing cells within the same population [8,9]. More than three nuclear criteria of malignancy should be present in most of the cellular population to classify the process as malignant since changes in the cytoplasm are not as reliable as nuclear ones.

Cytology analysis in general, and specifically nuclear criteria of malignancy, is considered to carry a degree of cytologist-dependent subjectivity [8,9]. To introduce a more quantifiable criterion, it is suggested that certain nuclear features observed under the microscope, captured in photographs, could be identified as particles due to their intranuclear heterogeneity. Consequently, malignant neoplasm nuclei are expected to exhibit a higher particle count compared to benign neoplasm nuclei, reflecting their increased nuclear criteria of malignancy. To explore this concept further, cytology preparations from samples of a neurofibroma and a fibrosarcoma are considered. The slides containing the samples were stained with Giemsa. Initial microscopic evaluation involved lower magnification objectives (4x and 10x) to assess sample quality and staining. Subsequent individual cell assessment and comparison were performed using the 40x objective, while the 100x immersion objective facilitated detailed observation of organisms, inclusions, and certain cellular characteristics.

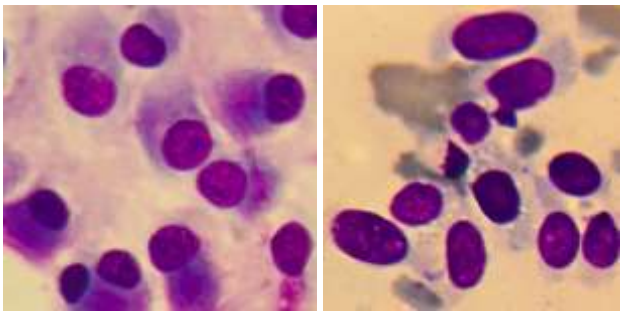

Figure 3: Typical images from Neurofibroma nuclei (left) and Fibrosarcoma nuclei (right) received at the Guernica Veterinary Clinic in the South Zone of Greater Buenos Aires, Argentina,

Figure 3 shows typical images from a cytology study. The image on the left side of Fig.3 corresponds to a 12-year-old male mixed-breed dog that presents a subcutaneous neoformation on the neck. The cytology diagnosis indicated a tumor of mesenchymal cells. The diagnosis of benign neurofibroma was confirmed by histopathological study. On the other hand, the image on the right side of Fig.3 corresponds to a 6-year-old female cat, common European breed, presented with a subcutaneous neoformation in the hip region. The cytology diagnosis indicated a tumor of mesenchymal cells with malignant characteristics. The diagnosis of fibrosarcoma was confirmed by histopathological study.

4 Results on Particles identification

In this study, we consider neurofibroma and fibrosarcoma cytology samples for the application of the method presented in section 2. A number of representative photos of a neurofibroma at 100x and of a fibrosarcoma at 100x were chosen. Fifteen nuclei images were obtained from the samples of each type of tumor with the aim of analyzing whether there is a significant difference between the quantities of particles for each type. Each of the nuclei images was processed separately, decomposing it into 4 component BIMF images. Then, the particles are detected in each of them, and the size measured as described above.

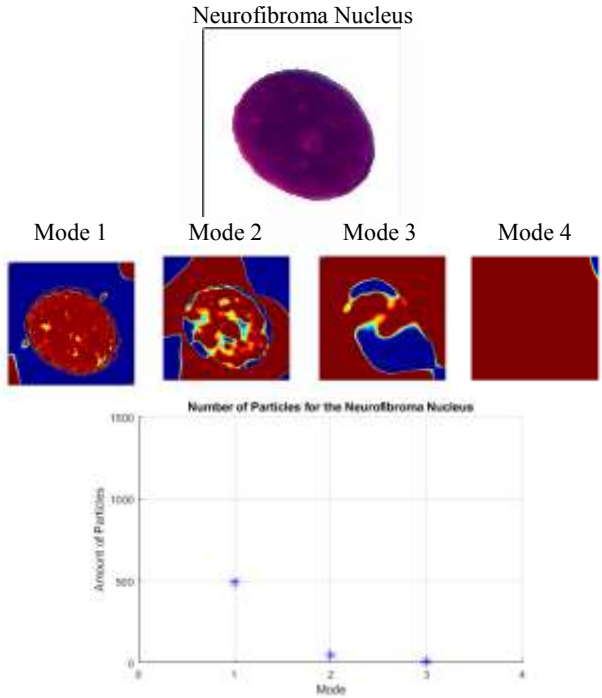

Figure 4: Neurofibroma nucleus, its four BIMFs and quantities of particles.

In Fig. 4 and Fig. 5 it is shown a nucleus of neurofibroma and a nucleus of fibrosarcoma, respectively, with their four bidimensional mode decomposition matrices and the number of particles found in each mode. It is observed that BIMF1 shows a more complex structure than the other image

modes. Hence, it is expected that most of the smaller particles will be found in mode 1.

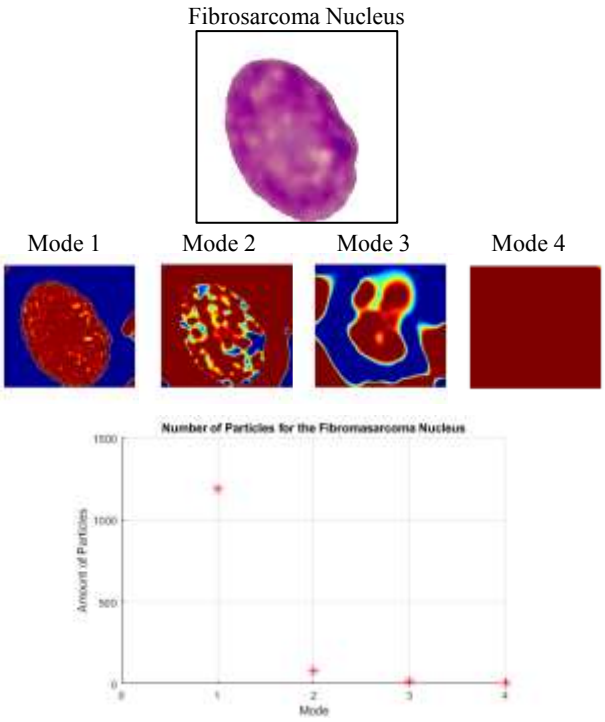

Figure 5: Fibrosarcoma nucleus, its four BIMFs and quantities of particles.

The number of particles identified in each component image was counted and the results obtained are plotted as star points in Fig. 6 and shown in Table 1 for the 15 nuclei.

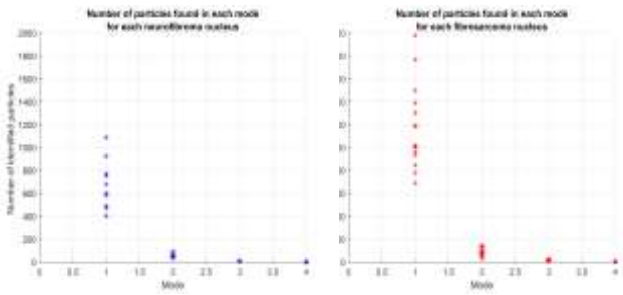

Figure 6: Number of particles found in each bidimensional image mode matrix. Neurofibroma (left) and Fibrosarcoma (right).

A tendency is observed where the number of particles for fibrosarcoma nuclei exceeds that of neurofibroma nuclei. The difference is particularly evident in mode 1, where the higher number of particles are found, since the smallest particles are captured in this mode. Notice that points are collapsed particularly at the higher modes meaning that a similar number of particles are found in these modes.

	Neurofibroma				Fibrosarcoma			
Nucleus	Mode 1	Mode 2	Mode 3	Mode 4	Mode 1	Mode 2	Mode 3	Mode 4
1	404	50	5	2	689	49	10	6
2	472	36	9	4	779	31	5	0
3	490	49	6	0	846	93	11	3
4	490	49	6	0	935	65	10	3
5	584	58	7	3	959	100	16	5
6	602	57	11	3	1002	57	10	0
7	679	47	7	3	1009	49	8	4
8	679	47	7	3	1019	58	12	4
9	754	66	12	3	1186	108	6	3
10	754	66	12	3	1190	78	13	4
11	770	54	12	3	1303	129	25	5
12	923	94	9	5	1389	84	9	4
13	923	94	9	5	1498	74	18	6
14	1088	91	12	4	1767	139	28	7
15	1088	91	12	4	1978	146	21	6

Table 1: Ordered number of particles found in each Neurofibroma (left) and Fibrosarcoma (right) BIMF.

The total number of particles in each nucleus was obtained by adding the partial amount from each image mode. Fig. 7 shows the quantities of particles ordered from smallest to largest, for the 15 nuclei of the neurofibroma and the 15 nuclei of the fibrosarcoma. The results obtained suggest a potential difference in the cellular characteristics between fibrosarcoma and neurofibroma nuclei. The fact that the particle number of fibrosarcoma nuclei exceeds that of neurofibroma nuclei implies that there may be a higher level of nuclear complexity in fibrosarcoma compared to neurofibroma.

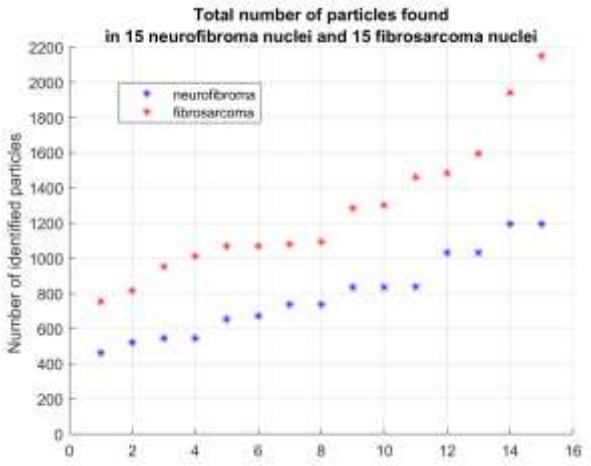

Figure 7: Total number of particles found in Neurofibroma nuclei and Fibrosarcoma nuclei.

It's worth noting that some neurofibroma nuclei have a greater number of particles than certain fibrosarcoma nuclei, indicating that the particle count in a particular nucleus is not decisive. Therefore, it's crucial not only to consider the quantity of cells for analysis but also their representativeness in the underlying biological process. Hence, the expertise

of a veterinarian specialized in cytology is still necessary for achieving proper sampling.

The findings obtained through the proposed algorithm are extremely valuable and could have implications for diagnosis, prognosis and treatment planning, since they can help distinguish between these two types of tumors according to their cytological characteristics. Additional analysis will be performed on a larger number of samples to obtain more robust and accurate statistics.

5 Conclusion

In this work we present a methodology for image analysis based on mode decomposition. We have described a simple and useful technique for particle identification, together with a size and morphology determination.

The proposed method was applied to images from cytological studies, corresponding to a benign tumor (neurofibroma) and a malignant tumor (fibrosarcoma). The results are promising indicating that this method can be a valuable tool for veterinarians and could provide valuable insights into the underlying biological differences between these tumors. More studies will be conducted with a larger number of samples to obtain more robust and accurate statistical information on this particular topic.

References:

[1] Clausel M., Oberlin T., Perrier V., The monogenic synchrosqueezed wavelet transform: a tool for the decomposition/demodulation of AM–FM images. *Applied and Computational Harmonic Analysis*. Vol. 39, Issue 3, 2015, pp 450-486.

[2] Cowell, R. L., Tyler, R. D., Meinkoth, J. H., & DeNicola, D. B. *Diagnostic cytology and hematology of the dog and cat-E-book*. Elsevier Health Sciences, 2007.

[3] De Buen de Argüero, Nuria. *Atlas de citopatología veterinaria*. Inter-Médica, Arg. 2014. ISBN: 978-950-555-423-2

[4] Ding H, Fu G, Yan Q, Jiang C, Cao T, Li W, Hu S, Xiao C., Deep attentive style transfer for images with wavelet decomposition. *Information Sciences*, Vol.587, 2022, pp 63-81.

[5] Dong H., Nie Y., Cui J., Kou W., Zou M., Han J., Guan X., Yang Z., A wavelet-based learning approach assisted multiscale analysis for estimating the effective thermal conductivities of particulate composites. *Computer Methods in Applied Mechanics and Engineering*, Vol. 374, 2021, p. 113591.

[6] Gogolewski D., Fractional spline wavelets within the surface texture analysis. *Measurement* 179, 2021, p. 109435.

[7] Kim D, Park M, Oh H-S., Bidimensional Statistical Empirical Mode Decomposition. *IEEE Signal Processing Letters*, 19(4), 2012, pp. 191-194.

[8] Mandarim-de-Lacerda, C. A., The Morphological Challenge in Determining Nuclear Size and Shape in Anatomopathological Neoplasia Analysis. *Int. Journal of Morphology*, *40*(3), 2022, pp. 683-687.

[9] Meachem, M.D., Burgess, H.J., Davies, J.L., & Kidney, B.A., Utility of nuclear morphometry in the cytologic evaluation of canine cutaneous soft tissue sarcomas. *Journal of Veterinary Diagnostic Investigation*, *24*(3), (2012), pp. 525-530.

[10] Muszkats JP, Muszkats SR, Zitto ME, Piotrkowski R, A statistical analysis of causal decomposition methods applied to Earth system time series. *Physica A*: Statistical Mechanics and its Applications. Vol 641. 2024, 129708.

[11] Nunes, J.C.; Bouaoune, Y.; Delechelle, E.; Niang, O.; Bunel, P. Image analysis by bidimensional empirical mode decomposition. *Image Vis. Comput.*, 21, 2003, 1019–102

[12] Nunes, Jean-Claude & Niang, Oumar & Yasmina, Bouaoune & Deléchelle, Eric & Bunel, Philippe. Texture analysis based on the bidimensional empirical mode decomposition with gray-level co-occurrence models. Proceedings - 7th International Symposium on Signal Processing and Its Applications, ISSPA 2003. 2, pp. 633 – 635 vol.2. 10.1109/ISSPA.2003.1224962.

[13] Oyelade O.N., Ezugwu A.E., A novel wavelet decomposition and transformation convolutional neural network with data augmentation for breast cancer detection using digital mammogram. *Science Report*, Vol.12, 2022, p. 5913.

[14] Sasikanth. Bi dimensional Empirical Mode Decomposition (BEMD), MATLAB Central File Exchange. Retrieved April 19, 2023.

[15] Shao Y., Du S., Tang H., An extended bi-dimensional empirical wavelet transform based filtering approach for engineering surface separation using high definition metrology. *Measurement* 178, 2021, p. 109259.

[16] Veluppal A., Sadhukhan D., Gopinath V., Swaminathan R., Differentiation of Alzheimer conditions in brain MR images using bidimensional multiscale entropy-based texture

analysis of lateral ventricles, *Biomedical Signal Processing and Control*, Vol.78. 2022, p. 103974.

[17] Xie Q., Hu J., Wang X., Du Y., Qin H., Novel optimization-based bidimensional empirical mode decomposition. *Digital Signal Processing*, Vol. 133, 2023, p. 103891.

[18] Yang L., Zhang M., Cheng J., Zhang T., Lu. F., Retina images classification based on 2D empirical mode decomposition and multifractal analysis. *Heliyon*, Vol.10, Issue 6, 2024, p. e27391.

[19] Yu J., Cheng X., Lu L., Wu B., A machine vision method for measurement of machining tool wear. *Measurement* 182, 2021, p. 109683.

Contribution of Individual Authors to the Creation of a Scientific Article (Ghostwriting Policy)

Marcela Morvidone, Diana Rubio and Rosa Piotrkowski formulated the problem and wrote the article.

Marcela Morvidone and Diana Rubio carried out the numerical simulations.

Diana Rubio and Nicolas Sassano designed the application of the technique to cytology images.

Nicolas Sassano provided the images and analyzed the results.

Sources of Funding for Research Presented in a Scientific Article or Scientific Article Itself

No funding was received for conducting this study.

Conflict of Interest

The authors have no conflicts of interest to declare that are relevant to the content of this article.